Journal of Medicinal Chemistry

Article

pubs.acs.org/jmc

Design, Synthesis, and Pharmacological Characterization of Novel Endomorphin-1 Analogues as Extremely Potent μ-Opioid Agonists

Xin Liu,‡ Yuan Wang,‡ Yanhong Xing,‡ Jing Yu, Hong Ji, Ming Kai, Zilong Wang, Dan Wang, Yixin Zhang, Depeng Zhao, and Rui Wang*

Key Laboratory of Preclinical Study for New Drugs of Gansu Province, School of Basic Medical Sciences, and Institute of Biochemistry and Molecular Biology, Lanzhou University, Lanzhou, 730000, P. R. China

Supporting Information

ABSTRACT: Recently we reported the synthesis and structure−activity study of endomorphin-1 (EM-1) analogues containing novel, unnatural α-methylene-β-aminopropanoic acids (Map). In the present study, we describe new EM-1 analogues containing Dmt[1], (*R*/*S*)-βPro[2], and (ph)Map[4]/(2-furyl)Map[4]. All of the analogues showed a high affinity for the μ-opioid receptor (MOR) and increased stability in mouse brain homogenates. Of the new compounds, Dmt[1]-(*R*)-βPro[2]-Trp[3]-(2-furyl)Map[4] (analogue **12**) displayed the highest affinity toward MOR, in the picomolar range (K_i^{μ} = 3.72 pM). Forskolin-induced cAMP accumulation assays indicated that this analogue displayed an extremely high agonistic potency, in the subpicomolar range (EC_{50} = 0.0421 pM, E_{max} = 99.5%). This compound also displayed stronger in vivo antinociceptive activity after iv administration when compared to morphine in the tail-flick test, which indicates that this analogue was able to cross the blood−brain barrier.

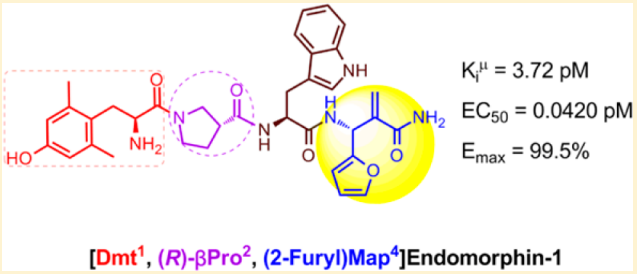

INTRODUCTION

Pain remains a major clinical problem and is the subject of intense medicinal research. The ubiquitous loss of quality of life experienced by patients with either acute or chronic pain has led to the development of various drugs to treat pain. The opioid system is one of the most studied pharmacological systems involved in pain systems modulation and consists of three subtypes of receptors: the μ-opioid receptor (MOR), the δ-opioid receptor (DOR), and the κ-opioid receptor (KOR).[1,2] Opioid agonists have long been employed as therapeutic agents for the treatment of moderate-to-severe pain. However, long-term use of the opioids carries the risk of numerous side effects, including acute tolerance, physical dependence, respiratory depression, constipation, nausea, and diverse gastrointestinal effects.[3] Therefore, the development of new therapeutics with useful analgesic properties and attenuated or eliminated side effects is a major goal in the clinical treatment of pain.

Many peptides are potential neuropharmaceuticals, and the study of naturally occurring opioid peptides provides a rational and potentially powerful approach to the design of novel analgesic therapeutics.[4] Endomorphin-1 (EM-1, H-Tyr[1]-Pro[2]-Trp[3]-Phe[4]-NH_2) and endomorphin-2 (EM-2, H-Tyr[1]-Pro[2]-Phe[3]-Phe[4]-NH_2) are endogenous opioid peptides isolated from the bovine brain and exhibit the highest selectivity and affinity for the MOR of all the endogenous peptides identified to date.[5−7] Notably, EMs are thought to inhibit pain signals without some of the undesirable side effects produced by morphine. In particular, the rewarding effect of EMs can be separated from the analgesic effect,[8] and they are less likely to induce respiratory depression and cardiovascular effects at effective antinociceptive doses.[9] Hence, EMs have attracted considerable interest since their discovery.[10,11] However, the pharmacological utility of these peptides faces many challenges in the drug development process, including their short duration of action, poor metabolic stability, and relative inability to cross the blood−brain barrier (BBB).[12−14] One of the major limitations to the use of EMs as analgesic drugs is their susceptibility to proteolysis. Because the opioid receptors are membrane−bound proteins, their ligands have to reach the target tissue and compete for binding within the extracellular space to exert their action.[15] However, many proteases are membrane−bound and have active sites facing the extracellular side. As a result, the opioid peptides undergo rapid degradation leading to the loss of physiological activity. A further challenge in the clinical development of EMs is their inability to effectively penetrate the BBB and gain access to the central nervous system (CNS). Many chemical modifications to EMs have been made in attempts to overcome the problems of enzymatic degradation and inability to cross the BBB, such as incorporation of unnatural amino acids, structural constraints, N-methylation of amino acids, quaternization of basic nitrogens, and alteration of lipophilicity.[10,11,16]

Structurally, EMs consist of both a "message" and an "address" domain. It is considered that Tyr-Pro-Trp/Phe and Phe-NH_2 correspond to the message and address fragments,

Received: February 7, 2013
Published: March 11, 2013

   dx.doi.org/10.1021/jm400195y | J. Med. Chem. 2013, 56, 3102−3114

respectively.[17,18] It is generally thought that the aromatic amino acids of opioid peptides are essential structural elements for receptor binding and activation. The message domain is considered important for ligand recognition: Tyr[1] is regarded as the most conserved residue for opioid activity, the aromatic amino acid residue in position 3 is the defining structural determinant between EM-1 and EM-2, and Pro[2] is thought to be a spacer residue that joins the two pharmacophore residues Tyr[1] and Trp[3]/Phe[3].[19,20] The address domain, which contains the C-terminal residue, is responsible for biological response and receptor selectivity.[21,22]

Many EM-based compounds have been designed and synthesized to explore the importance of specific residues and to gain an insight into the structural requirements for bioavailability.[23−28] A particularly successful modification that results in the enhancement of MOR affinity is the incorporation of substituents in the aromatic ring of Tyr[1] to obtain more hydrophobic amino acids, such as 2′6′-dimethyltyrosine (Dmt), which was shown to dramatically increase receptor affinity in numerous peptides and to enhance their antinociceptive effect.[29,30] β-Amino acids are an interesting class of residues for studying the structure−activity relationship (SAR) of EMs, and in some cases, the replacement of α-amino acids with β-amino acids results in improved activity.[31−33] It has been reported that the replacement of Pro[2] with alicyclic β-amino acids, such as β-proline,[34,35] piperidine-3-carboxylic acid (Nip),[36] and azetidine-3-carboxylic acid (3Aze),[37] leads to compounds with increased affinity for the MOR. Furthermore, the introduction of β-amino acids usually improves the metabolic stability of the peptide.[38−40] Recently, we reported a new series of unnatural β-amino acids known as α-methylene-β-amino acids (Map).[41] SAR studies have demonstrated that when incorporated at position 4 of EM-1, residue (ph)Map and (2-furyl)Map increase the biological activity of the peptide.

In the present study, in an effort to improve bioactivity and stability, a series of EM-1 analogues were synthesized by employing a combination of chemical modifications. Dmt, (*R*/*S*)-β-Pro, (ph)Map, and (2-furyl)Map were used to replace the corresponding natural amino acids of EM-1. The structures of the unnatural amino acids that were incorporated into EM-1 are shown in Figure 1. The opioid receptor affinity and selectivity

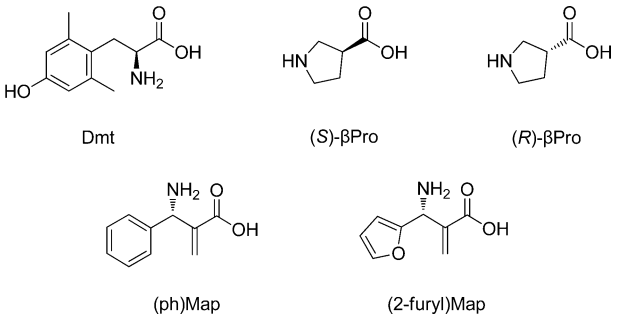

Figure 1. Structures of unnatural amino acids incorporated into endomorphin-1.

of these analogues was determined by radioligand binding experiments and by GPI/MVD bioassays. The biological functionality of the analogues was then assessed in cyclic AMP accumulation and ERK1/2 phosphorylation assays. Molecular modeling approaches were employed to gain more insight into the structure−activity relationship between the ligands and the MOR. The degradation rates of the analogues were then evaluated in the presence of mouse brain homogenate. We further characterized their in vivo activity using the tail-flick test after both intracerebroventricular (icv) and intravenous (iv) administration in mice.

RESULTS

Chemistry. All standard amino acids, Dmt, and (*R*/*S*)-β-Pro were commercially available, while the chiral 2-methylene-3-amino propanoic acids (Map) were prepared in the manner previously reported by us.[41,42] All of the analogues were obtained using solution-phase methods with a segment-coupling peptide synthesis strategy. Synthesis of the analogues was conducted by performing an active ester reaction, and EDC and HOBt were used as coupling agents. The established peptides were then purified using semipreparative RP-HPLC and characterized by RP-HPLC, TLC, ESI-TOF MS, and mp. Purities were determined to be 95−99% as characterized by analytical RP-HPLC. The detailed analytical properties of the synthetic analogues are provided in Table 1.

Receptor Binding Affinity. The affinity and selectivity of the EM-1 analogues were evaluated by radioligand binding assays using whole-cell preparations from HEK293 cells expressing either MOR, DOR, or KOR. Analogues **1** and **2**, which we have described previously, were also characterized for comparative purpose.[41] As shown in Table 2, compared with analogue **1**, replacement of the Pro[2] with (*S*)-β-Pro[2] gave analogue **3** a 10-fold increased DOR affinity, but it retained a similar MOR affinity to analogue **1**. The introduction of (*S*)-β-Pro[2] into analogue **4** resulted in a decreased affinity for both MOR and DOR. For analogues **5** and **6**, in which (*R*)-β-Pro[2] was incorporated, improved MOR affinities were observed when compared with their (*S*)-stereoisomer correlate (1.9-fold and 4.6-fold, respectively). The replacement of Tyr[1] with Dmt[1] greatly increased MOR affinity but also decreased the MOR selectivity of the analogues. Analogues **7** and **8** exhibited high MOR affinities, but their DOR affinities increased dramatically; as a result, they were the least MOR selective analogues among of all the synthesized peptides described here. The subsequent modification, performed at position 2 with (*S*)-β-Pro, afforded analogues **9** and **10** with 2.4-fold and 3.2-fold increased MOR affinities, respectively. Coapplication of Dmt[1], (*R*)-β-Pro[2], and (ph)Map[4]/(2-furyl)Map[4] resulted in analogues **11** and **12** having the highest MOR affinities, in the picomolar range (K_i^{μ} = 9.86 pM and 3.72 pM, respectively), with their DOR affinities being comparable to those of analogues **9** and **10**. The analogues containing Dmt[1] were also assayed for their affinity for KOR. As shown in Table 2, the tested analogues (**7**−**12**) showed relatively low affinities for KOR, in the submicromolar range (from 174 to 240 nM).

In Vitro Pharmacological Activity. The in vitro activities of the analogues were examined by assessing their ability to inhibit electrically evoked neurotransmitter release and the subsequent muscle contractions in guinea pig ileum (GPI) and mouse vas deferens (MVD) preparations (Table 2). The GPI assay is generally considered representative of MOR interactions, but the preparation also contains KOR, whereas the predominant receptor subtype in the MVD tissue is DOR, with MOR and KOR also being present at low levels. In the GPI assays, all analogues exhibited increased potencies over EM-1. In agreement with the radioligand binding results, analogues with Tyr[1] showed low nanomolar GPI activity, while Dmt[1] substitution afforded the analogues with subnanomolar potencies. It is noteworthy that, in radioligand binding assays,

dx.doi.org/10.1021/jm400195y | J. Med. Chem. 2013, 56, 3102−3114

Table 1. Analytical Data for EM-1 Analogues

		TOF MS $[M + H]^+$				
no.	sequence	calcd	found	RP HPLC[a] (min)	mp (°C)	purity[b] (%)
3	Tyr-(*S*)-*β*Pro-Trp-(ph)Map-NH_2	623	623.3019	14.116	139−141	98
4	Tyr-(*S*)-*β*Pro-Trp-(2-furyl)Map-NH_2	613	613.2803	14.332	137−139	99
5	Tyr-(*R*)-*β*Pro-Trp-(ph)Map-NH_2	623	623.3008	14.380	132−135	98
6	Tyr-(*R*)-*β*Pro-Trp-(2-furyl)Map-NH_2	613	613.2804	14.328	133−135	98
7	Dmt-Pro-Trp-(ph)Map-NH_2	651	651.3324	14.479	142−145	97
8	Dmt-Pro-Trp-(2-furyl)Map-NH_2	641	641.3090	14.433	147−149	98
9	Dmt-(*S*)-*β*Pro-Trp-(ph)Map-NH_2	651	651.3325	14.313	142−145	96
10	Dmt-(*S*)-*β*Pro-Trp-(2-furyl)Map-NH_2	641	641.3106	14.659	151−153	96
11	Dmt-(*R*)-*β*Pro-Trp-(ph)Map-NH_2	651	651.3319	14.185	151−153	97
12	Dmt-(*R*)-*β*Pro-Trp-(2-furyl)Map-NH_2	641	641.3120	13.903	150−153	99

[a] t_R with Delta-Park C18 column (4.6 mm ×250 mm, 5 μm), A:B = 10:90 to A:B = 90:10 for 30 min, A:B = 90:10 to A:B = 10:90 for 5 min. [b] Purity determination based on analytical RP-HPLC.

Table 2. Opioid Receptor Binding Affinities and in Vitro Pharmacological Activity of EM-1 and Analogues

						IC_{50} (nM)[e]	
no.	peptide	K_i^μ (nM)[a,d]	K_i^δ (nM)[b,d]	K_i^κ (nM)[c,d]	K_i ratio $\mu/\delta/\kappa$	GPI	MVD
0[f]	Tyr-Pro-Trp-Phe-NH_2	2.60 ± 0.21	6080 ± 640	–	1/2338/–	14.1 ± 1.7	30.4 ± 2.6
1[f]	Tyr-Pro-Trp-(ph)Map-NH_2	0.535 ± 0.076	56010 ± 5180	–	1/104692/–	6.81 ± 0.80	7.53 ± 1.22
2[f]	Tyr-Pro-Trp-(2-furyl)Map-NH_2	0.221 ± 0.014	50010 ± 2880	–	1/226290/–	2.92 ± 0.31	15.8 ± 0.9
3	Tyr-(*S*)-*β*Pro-Trp-(ph)Map-NH_2	0.574 ± 0.072	5580 ± 350	–	1/9721/–	3.21 ± 0.77	4.89 ± 0.97
4	Tyr-(*S*)-*β*Pro-Trp-(2-furyl)Map-NH_2	0.758 ± 0.047	6950 ± 810	–	1/9169/–	8.12 ± 1.51	4.90 ± 0.88
5	Tyr-(*R*)-*β*Pro-Trp-(ph)Map-NH_2	0.296 ± 0.028	2810 ± 130	–	1/9493/–	1.82 ± 0.71	2.28 ± 0.52
6	Tyr-(*R*)-*β*Pro-Trp-(2-furyl)Map-NH_2	0.165 ± 0.017	2780 ± 150	–	1/16848/–	1.67 ± 0.67	2.91 ± 1.16
7	Dmt-Pro-Trp-(ph)Map-NH_2	0.0322 ± 0.0052	25.6 ± 3.5	192 ± 9	1/795/5963	0.467 ± 0.124	0.556 ± 0.118
8	Dmt-Pro-Trp-(2-furyl)Map-NH_2	0.0405 ± 0.0180	22.2 ± 3.3	200 ± 17	1/548/4938	0.767 ± 0.201	0.533 ± 0.083
9	Dmt-(*S*)-*β*Pro-Trp-(ph)Map-NH_2	0.0137 ± 0.0002	18.9 ± 1.9	240 ± 18	1/1380/17518	0.539 ± 0.143	1.53 ± 0.49
10	Dmt-(*S*)-*β*Pro-Trp-(2-furyl)Map-NH_2	0.0128 ± 0.0019	30.4 ± 3.2	180 ± 17	1/2375/14063	0.834 ± 0.223	0.962 ± 0.271
11	Dmt-(*R*)-*β*Pro-Trp-(ph)Map-NH_2	0.00986 ± 0.0010	27.3 ± 1.2	174 ± 17	1/2769/17647	0.226 ± 0.089	0.406 ± 0.071
12	Dmt-(*R*)-*β*Pro-Trp-(2-furyl)Map-NH_2	0.00372 ± 0.00063	19.8 ± 2.2	205 ± 10	1/5323/55108	0.167 ± 0.059	0.548 ± 0.092

[a] Displacement of [^{3}H]DAMGO (K_d = 0.6 nM, *μ*-selective). [b] Displacement [^{3}H]DPDPE (K_d = 2.8 nM, *δ*-selective). [c] Displacement [^{3}H]U69,593 (K_d = 2.9 nM, *κ*-selective). [d] Displacement was done using whole cell preparations from transfected HEK293 cells expressing *μ*-opioid receptor, *δ*-opioid receptor, and *κ*-opioid receptor, respectively. K_i values were calculated according to the Cheng−Prusoff equation: $K_i = EC_{50}/(1 + [\text{ligand}]/K_d)$, where the shown K_d values were taken from isotope saturation experiments. Data are expressed as the mean ± SEM, $n \geq 3$, each performed in triplicate. [e] Values represent the average of 10−15 measurements. [f] Values were cited from our previous report.[41]

Table 3. Functional Activity of EM-1 and Analogues[a]

		μ-OR		*δ*-OR	
no.	sequence	EC_{50}(nM)	E_{max} (%)	EC_{50}(nM)	E_{max} (%)
0[b]	Tyr-Pro-Trp-Phe-NH_2	14.4 ± 0.6	83.1 ± 4	–	–
1[b]	Tyr-Pro-Trp-(ph)Map-NH_2	0.160 ± 0.090	97.9 ± 3	–	–
2[b]	Tyr-Pro-Trp-(2-furyl)Map-NH_2	0.0334 ± 0.0012	97.1 ± 5	–	–
3	Tyr-(*S*)-*β*Pro-Trp-(ph)Map-NH_2	0.0570 ± 0.0036	95.5 ± 3	–	–
4	Tyr-(*S*)-*β*Pro-Trp-(2-furyl)Map-NH_2	0.0933 ± 0.0051	94.9 ± 4	–	–
5	Tyr-(*R*)-*β*Pro-Trp-(ph)Map-NH_2	0.0397 ± 0.0029	96.8 ± 4	–	–
6	Tyr-(*R*)-*β*Pro-Trp-(2-furyl)Map-NH_2	0.00853 ± 0.00092	96.2 ± 6	–	–
7	Dmt-Pro-Trp-(ph)Map-NH_2	0.000130 ± 0.000003	97.2 ± 3	51.6 ± 1.8	77.5 ± 5
8	Dmt-Pro-Trp-(2-furyl)Map-NH_2	0.000516 ± 0.000045	96.5 ± 4	48.9 ± 1.9	76.3 ± 3
9	Dmt-(*S*)-*β*Pro-Trp-(ph)Map-NH_2	0.000107 ± 0.000001	97.1 ± 6	40.4 ± 2.8	77.6 ± 6
10	Dmt-(*S*)-*β*Pro-Trp-(2-furyl)Map-NH_2	0.000109 ± 0.000007	98.6 ± 2	47.3 ± 2.1	72.2 ± 3
11	Dmt-(*R*)-*β*Pro-Trp-(ph)Map-NH_2	0.0000912 ± 0.0000092	98.9 ± 5	47.9 ± 2.9	72.1 ± 3
12	Dmt-(*R*)-*β*Pro-Trp-(2-furyl)Map-NH_2	0.0000420 ± 0.0000056	99.5 ± 3	89.3 ± 3.3	73.8 ± 5
DAMGO	Tyr-D-Ala-Gly-NMe-Phe-Gly-ol	3.04 ± 0.32	98.1 ± 6		
DPDPE	Tyr-c(D-Pen-Gly-Phe-D-Pen)-OH			0.557 ± 0.043	87.4 ± 3

[a] Effects of peptides on forskolin stimulated cyclic AMP accumulation by *μ*-/*δ*-opioid receptor. HEK293 cells expressing MOR or DOR were stimulated with increasing concentrations of the indicated peptides as described in Experimental Section. EC_{50} and E_{max} values were calculated by using the GraphPad Prism software. Data are expressed as the mean ± SEM, $n \geq 3$, each performed in triplicate. [b] Values were cited from our previous report.[41]

dx.doi.org/10.1021/jm400195y | J. Med. Chem. 2013, 56, 3102−3114

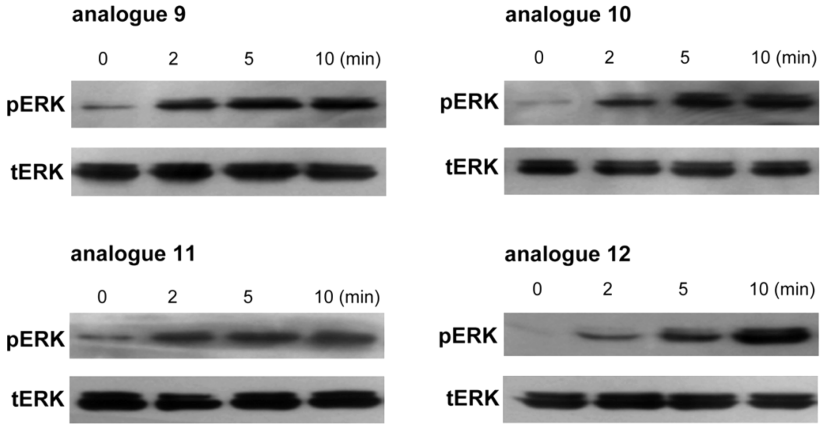

Figure 2. Stimulation of ERK1/2 phosphorylation in HEK293 cells expressing human μ-opioid receptor. HEK293 cells stably expressing μ-opioid receptor were treated with analogues. Whole cell lysates were prepared and analyzed for pERK and ERK content by Western blot. Results are representative of at least three independent experiments.

analogues **9** and **10** displayed similar MOR affinities, but in the GPI assay, analogue **9** displayed the higher potency. In the MVD assays, all analogues showed good MVD activity. Analogue **9** exhibited a relative lower potency than predicted by its DOR binding affinity. To clarify the receptor subtype specificity of the analogues, a specific DOR antagonist, naltrindole, was used in the MVD assay. We found that the inhibitory effect induced by the analogues in the MVD assay could only be partly antagonized by naltrindole, suggesting that the unexpectedly high MVD activities of the analogues were mainly mediated by the MORs that coexist in the MVD tissue. A similar discrepancy between MVD potency and DOR binding affinity has also been observed in previous studies.[41,43−45]

Cyclic-Adenosine Monophosphate (cAMP) Accumulation. To confirm the functional behavior of the peptide analogues, forskolin-stimulated [^{3}H]cAMP accumulation was evaluated in HEK293 cells expressing each of the three opioid receptors individually.[46,47] Each of the analogues inhibited forskolin (10 μM)-stimulated cAMP production in a concentration-dependent manner. Potency (EC_{50}) and efficacy (E_{max}) values were compared with those of DAMGO. As shown in Table 3, all of the analogues displayed potencies much higher than that of DAMGO. Analogues **1**−**5** exhibited potencies in the picomolar to subnanomolar range (EC_{50} = 39.7 pM to 0.160 nM). Combined substitution with both (*R*)-βPro^2 and (2-furyl)Map^4 (analogue **6**) resulted in a low picomolar potency (EC_{50} = 8.53 pM). No detectable DOR potency was observed in any of the analogues with the Tyr^1 residue (analogues **1**−**6**). The additional modification of replacing Tyr^1 with Dmt^1 produced a significant enhancement of MOR potency. Analogues **7**−**10** displayed subpicomolar potencies at MOR, ranging from 0.107 to 0.516 pM. Analogues **11** and **12** were the two most potent μ-agonists, with functional potencies in the two-digit femtomolar range (EC_{50} = 0.0912 pM and 0.0420 pM, respectively). It is notable that the incorporation of Dmt^1 also provided the analogues with nanomolar potencies at DOR (analogues **7**−**12**). It is well-known that DAMGO and DPDPE act as full agonists toward MOR and DOR, respectively.[48−50] All analogues exhibited high efficacies, comparable to that of DAMGO, confirming that these compounds are full agonists at MOR. Additionally, compared to DPDPE, analogues **7**−**12** showed lower efficacies and acted as partial agonists at DOR. None of the tested analogues showed any detectable activity toward KOR at a concentration of 10 μM.

ERK1/2 Phosphorylation. The ERK phosphorylation cascade is essential to MOR intracellular signaling.[51,52] Therefore, we next assessed the effects of the analogues on the activation of ERK1/2 in HEK293 cells expressing MOR. Analogues **9**−**12** were selected for this assay, taking into consideration of their high bioactivity. The cells were treated with analogues at a concentration of 1 μM, and incubated at 37 °C for 10 min. ERK1/2 activation was determined by the level of phosphorylation of the molecules. As shown in Figure 2 analogues **9**−**12** clearly stimulated ERK1/2 phosphorylation in a time-dependent manner. The four analogues were able to phosphorylate ERK1/2 via MOR within 2 min. This indicates that the analogues are capable of inducing ERK1/2 activation. The level of phosphorylation stimulated by analogues **9**−**12** was much stronger than that caused by EM-1,[41] indicating that these four analogues have higher potencies for ERK1/2 phosphorylation.

Metabolic Stability. To examine the resistance of the analogues to enzymatic hydrolysis, the selected analogues were treated in mouse brain membrane homogenate. RP-HPCL analysis was then used to determine the stability of the peptides. Table 4 summarizes the half-lives determined for EM-1 and some of its potent analogues. EM-1 experienced a rapid degradation with a half-life of 16.9 min. The analogues examined in this assay displayed a significantly enhanced resistance to enzymatic degradation, with half-lives exceeding 600 min.

Table 4. Half-Lives of EM-1 and Its Potent Analogues in Mouse-Brain Membrane Homogenate[a]

no.	half-life[b] (min)
1[c]	16.9 ± 1.2
9	>600
10	>600
11	>600
12	>600

[a]Values are arithmetic mean of at least three individual experiments ± SEM. The protein content of the brain homogenate was 2.1 mg/mL. [b]Half-lives were calculated on the basis of pseudo-first-order kinetics of the disappearance of the peptides. [c]Values were cited from our previous report.[41]

dx.doi.org/10.1021/jm400195y | J. Med. Chem. 2013, 56, 3102−3114

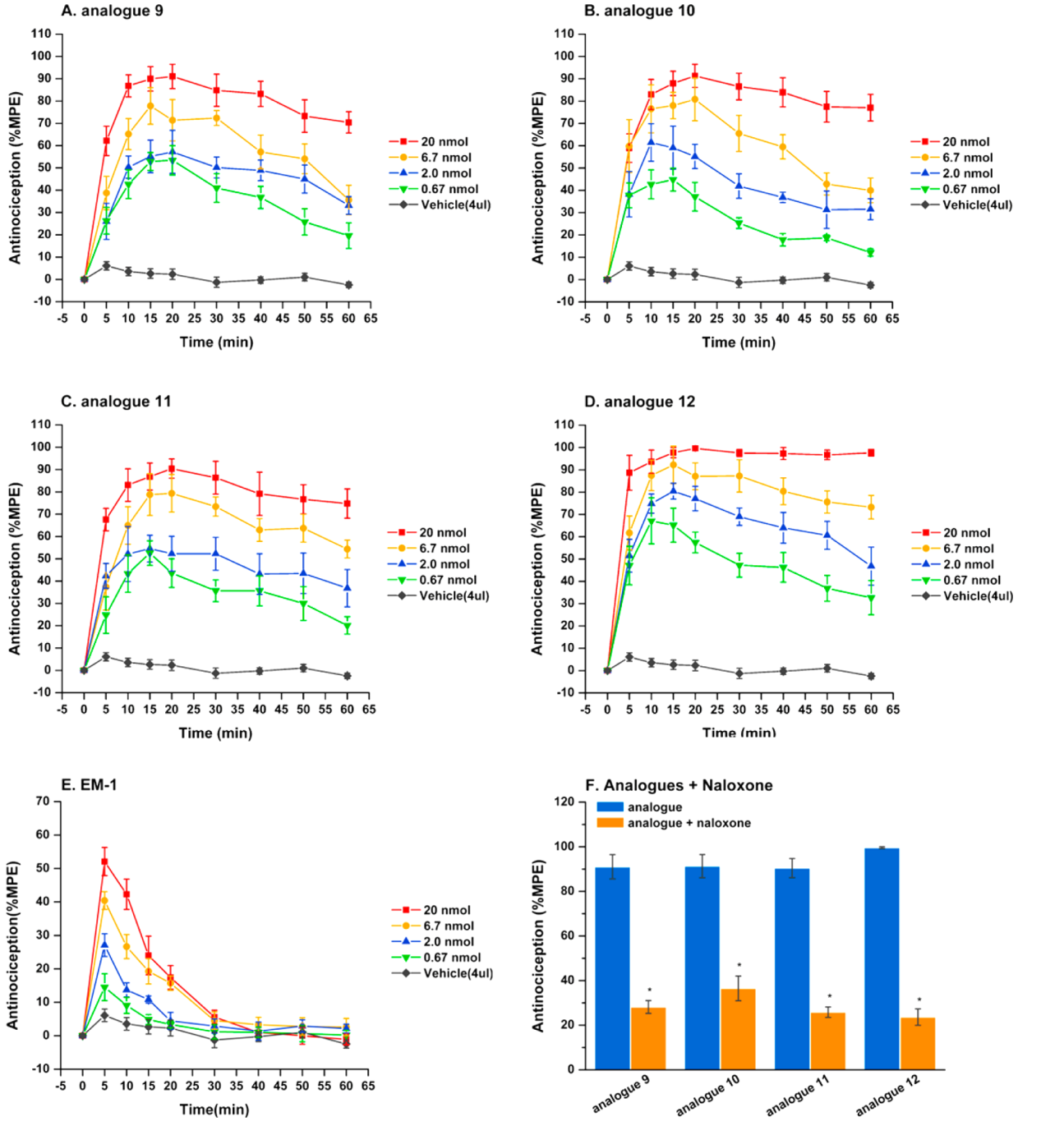

Figure 3. Tail-flick test versus time curves of the antinociceptive effect of analogues **9** (A), **10** (B), **11** (C), **12** (D), and EM-1 (E) after icv administration. The doses used are shown in the figure (nmol/kg). Each value represents the mean ± SEM for 10−15 mice. The icv injection vehicles versus each dose of the above drugs are significantly different ($p < 0.05$) (Student's t test). The antinociceptive effects induced by EM-1 analogues **9**−**12** at 20 nmol/kg are significantly antagonized by naloxone (2 mg/kg) ($p < 0.05$) (F). Naloxone was administered ip 10 min before icv administration of drugs. The error bar indicates the SEM of the mean, and the asterisk indicates that the response is significantly different from control.

Antinociception. The antinociceptive activities of analogues **9**−**12**, which displayed the highest binding affinities and functional activities, were assessed in the mouse tail-flick test after both icv and iv administration. As shown in Figure 3A−D, all of the analogues exhibited time- and dose-dependent inhibition and significant latency of tail-flick during the time course measured. Analogue **12** was the most potent with an ED_{50} value of 0.532 (0.421−0.678) nmol/kg. Analogues **9**, **10**, and **11** showed similar activities, with ED_{50} values of 0.779 (0.536−0.922) nmol/kg, 0.950 (0.715−1.080) nmol/kg, and 0.822 (0.589−1.147) nmol/kg, respectively. The analogues also produced much larger AUCs (area under the curve) than that produced by EM-1, as shown in Figure S2, Supporting Information. The icv activity of EM-1 was also included as a reference. Furthermore, the analgesic effects of the analogues were reliably reversed by naloxone (2 mg/kg, ip), indicating that their analgesic effect was mediated by opioid receptor (Figure 3F).

dx.doi.org/10.1021/jm400195y | J. Med. Chem. 2013, 56, 3102−3114

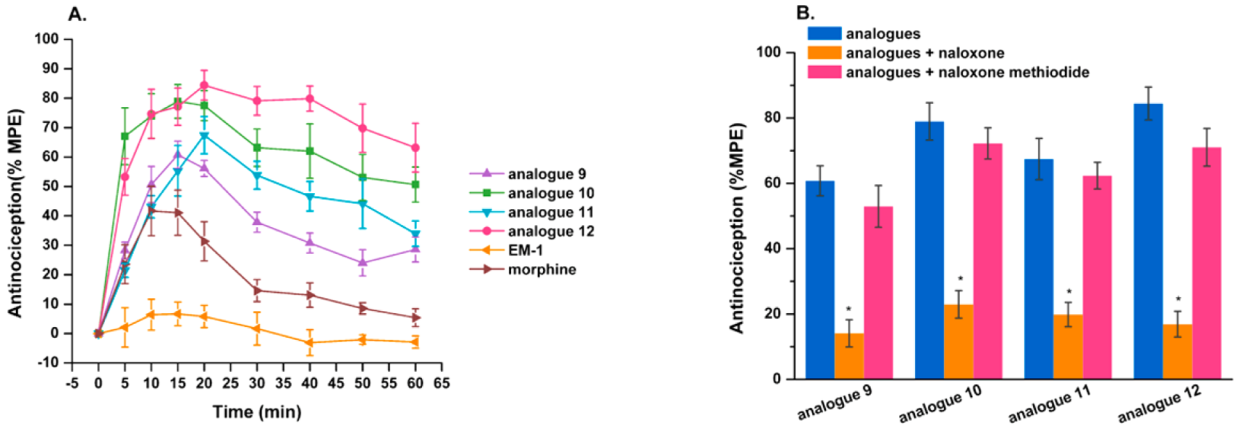

Figure 4. (A) Tail-flick test versus time curves of the antinociceptive effect of analogues **9**, **10**, **11**, **12**, EM-1, and morphine after iv administration. The dose used is 2 mg/kg. Each value represents the mean ± SEM for 8−10 mice. (B) Antagonism of antinociception elicited by 2 mg/kg iv analogues **9**−**12** in the tail-flick assay by naloxone (10 mg/kg ip, administered 10 min before drugs) and by naloxone methiodide (10 mg/kg ip, administered 10 min before drugs). The error bar indicates the SEM of the mean, and the asterisk indicates that the response is significantly different from control.

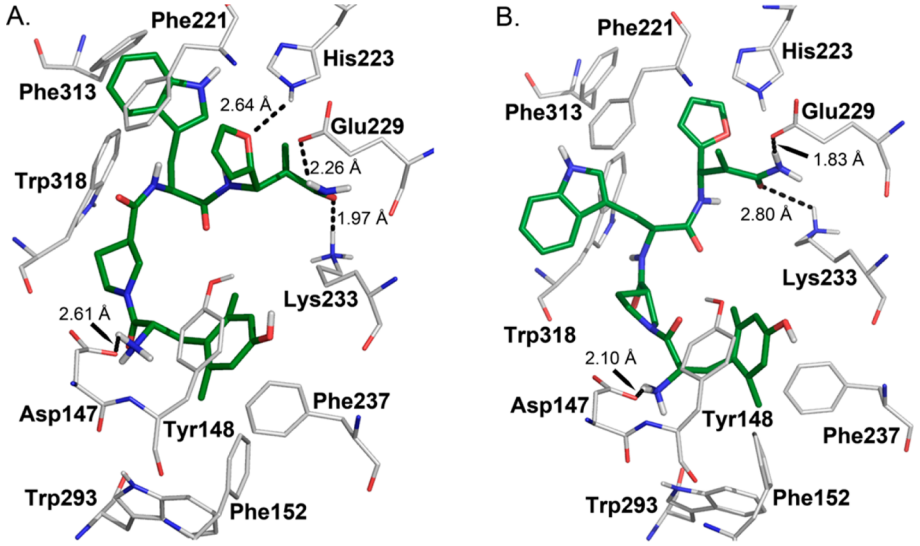

Figure 5. The binding poses of analogue **10** (A) and analogue **12** (B) after MD simulations optimization. The carbon atoms of the analogues and the receptor are colored in green and gray, respectively. Receptor residues making close interactions with the peptides are labled. Nitrogen, oxygen, and hydrogen atoms are colored in blue, red, and gray, respectively. Hydrogen bonds are represented as black dashed lines with measurement.

The antinociceptive effect of the four analogues after iv administration was studied. Morphine and EMs were used as positive control. The analgesia time response curves induced by morphine and the analogues are shown in Figure 4. Fifteen to twenty minutes after iv administration, the analogues tested reached their peak of activity, with the analgesic effect induced by these analogues, at a dose of 2 mg/kg being significantly stronger than that induced by morphine at the same dose. The duration of the analgesic effect was approximately 30 min for morphine and over 60 min for the analogues. The most potent analogue of the test compounds was analogue **12**, which induced a maximal antinociceptive effect of 84.4%. We then determined whether the opioid antagonists were able to inhibit the antinociceptive action of the analogues. As shown in Figure 4, the antinociceptive effects of the analogues were effectively reversed by ip injected naloxone (10 mg/kg). In contrast, naloxone methiodide (10 mg/kg, ip) did not alter the analgesic effect of iv administrated analogues. The AUCs produced by the analogues are shown in the Supporting Information (Figure S3).

Molecular Modeling. In view of their biological activities and structural diversity, analogues **10** and **12** were subjected to molecular docking and molecular dynamics (MD) simulations, in the hope of elucidating their specific binding features. In the established binding pose of analogue **12** (Figure 5B), the protonated moiety of Dmt[1] interacted with the carboxyl group of Asp147 to form a salt bridge. The side chain of Dmt[1] was also stabilized by several stacking interactions with Tyr148, Phe152, Phe237, and Trp293. The aromatic group of Trp[3] was inserted into the hydrophobic pocket between Phe221, Phe313, and Trp318. This analogue formed three hydrogen bonds with His223, Glu229, and Lys233, respectively. For analogue **10** (Figure 5A), Dmt[1] was involved in the same ligand−receptor interactions as those described for analogue **12**, and the hydrogen bonds with Glu229 and Lys233 were maintained. However, different binding modes of the two analogues were observed for the residues at positions 3 and 4. In analogue **12**,

dx.doi.org/10.1021/jm400195y | J. Med. Chem. 2013, 56, 3102−3114

the Trp[3] moiety oriented toward the upper part of the binding pocket, and the furyl ring of (2-furyl)Map[4] formed a hydrogen bond with His233. For analogue **10**, the aromatic group of Trp[3] was moved toward the transmembrane 7 (TM7) domain, showing a buried orientation of the side chain in the TM region; as a result, the interaction between (2-furyl)Map[4] and His223 was weakened, and the corresponding hydrogen bond was broken.

DISCUSSION

Several unnatural amino acids, such as Dmt, (*R*/*S*)-β Pro, (ph)Map, and (2-furyl)Map, were incorporated into EM-1 at appropriate positions. The bioactivity and stability of these analogues was then determined. In our previous report, we developed a new series of unnatural amino acids, 2-methylene-3-aminopropanoic acids (Map), and introduced these into the sequence of EM-1. We found that the peptides (ph)Map[4]-EM-1 and (2-furyl)Map[4]-EM-1 were the two most potent analogues, displaying 4-fold and 12-fold increased MOR affinity over EM-1, respectively; (2-furyl)Map[4]-EM-1 was 431 times more potent than EM-1 in the functional assays.[41] In the present study, the (2-furyl)Map[4]-containing analogues produced similar or better activities at the MOR compared with their (ph)Map[4] cognates. This finding is in agreement with our previous finding that (2-furyl)Map[4] substitution appeared to be more effective than (ph)Map[4] substitution for improving the opioid activity of EM-1. Our data also suggested that a heterocyclic ring, such as the furan ring, probably had an important application in opioid peptide engineering. Another biological feature of the (ph)Map[4]/(2-furyl)Map[4] modifications was that they significantly enhanced the MOR selectivity of the peptide. The DOR/MOR selectivity values of analogues **1**−**6** were all above 9000, indicating a strong MOR binding preference. Further modification of analogues **1**−**6**, employing Dmt[1], resulted in the expected increase of the MOR affinities for analogues **7**−**12** but at the same time decreased the MOR selectivity of these peptides. Dmt[1] substitution enhanced affinity for all three opioid receptor subtypes relative to the Tyr[1]-containing peptides, which resulted in the decreased selectivity of analogue containing Dmt[1].[29,53] However, it is notable that analogues **7** and **8**, the two least MOR-selective compounds, still displayed a robust binding preference for the MOR with selectivity values of 795 and 548, respectively. This result indicates that the effect of Dmt[1] replacement in decreasing the peptide's MOR selectivity was partially compensated by the introduction of (ph)Map[4] or (2-furyl)-Map[4].

The Pro residue at position 2 of EM-1 is regarded as a stereochemical spacer that fixes the aromatic side chain groups in their proper spatial orientation.[10,11] It has been demonstrated that the chiral configuration of Pro[2] is a key factor in determining the activity and selectivity of EMs. In our analysis of the binding and functional activities of the analogues, we found that the (*R*)-β Pro[2]-containing derivatives exhibited increased bioactivities at the MOR compared to those containing the corresponding (*S*)-β Pro[2] residue. This finding correlates well with those of previous studies that employed β Pro or its cyclic mimetics at position 2.[34−37] Our data confirms that the (*R*)-stereoisomer of β Pro appears to be a favorable configuration for MOR activity. In addition to its influence on binding activity, β Pro[2] also exerted a varied influence on receptor subtype selectivity. The replacement of Pro[2] with β Pro[2] afforded analogues **3**−**6** with a marked increase in their binding affinity for DOR, which consequently led to a dramatic loss of MOR selectivity. Consistent with previous findings, the introduction of β Pro mimetics resulted in decrease selectivity.[11] However, in contrast to previous findings, the incorporation of β Pro in analogues **9**−**12** led to an increase in MOR selectivity. Comparing the binding affinities of analogues **7** and **8** with those of analogues **9**−**12**, it appeared that these compounds exhibited similar binding potencies at DOR with varying potencies at MOR. In other words, when Dmt[1] and (ph)Map[4]/(2-furyl)Map[4] were incorporated into EM-1, the additional replacement of Pro[2] with R/S-β Pro[2] had only a minor impact on DOR affinity, but this modification induced an increase in MOR affinity. As a result, analogues **9**−**12** became more selective for the MOR. Such a tendency was also observed when we examined the KOR/MOR selectivity of our analogues. These results indicate that, compared with single point substitutions, β Pro[2] exhibits a different impact on ligand selectivity in a multiple-site modification.

To further investigate and compare the functional activities of our analogues at the opioid receptors, we examined forskolin-induced intracellular cAMP accumulation, and phosphorylation of ERK1/2 in HEK293 cells. The results of our functional assays paralleled those of the binding assays. All of the analogues acted as full agonists, and displayed very high potencies at the MOR. Notably, analogue **6** with Tyr[1] displayed a high potency for the MOR, in the picomolar range. Replacing the Tyr[1] of analogue **6** with Dmt[1] resulted in the extremely potent analogue **12**, with MOR potency in the subpicomolar range (EC_{50} = 0.042 pM). Because the Dmt[1]-containing analogues also displayed DOR affinities in the low nanomolar range, their functional activities at DOR were also measured by the cAMP accumulation assay. These analogues exhibited moderate potencies at DOR as partial agonists; however, considering their low DOR selectivities, we propose that the analogues containing Dmt[1] mainly exert their bioactivity through activation of the MOR. It has been reported that activation of the MOR enhances the signaling of ERK1/2, which might contribute to pain regulation.[54,55] Our ERK1/2 phosphorylation assay showed that all of the analogues tested elicited a significant increase in ERK1/2 phosphorylation at a concentration of 1 μM, which further confirms the agonistic properties of the analogues for the MOR.

Given that the majority of opioid peptides undergo rapid degradation, and thus limited delivery to the CNS, it is unlikely that these peptides would be clinically useful. Because our synthesized analogues displayed highly improved opioid activities and metabolic stabilities, the in vivo activity was next examined using the tail-flick test following both central and systemic administration. The icv activities of the tested analogues were in good agreement with the results of our radioligand binding and cAMP accumulation assays. The subsequent peripheral (iv) administration demonstrated that after iv injection, the tested analogues (2 mg/kg) produced an analgesic effect stronger than that of morphine. The most potent compound, analogue **12**, induced a strong and consistent analgesic effect during the experiment. The metabolic stability of the analogues appears to be an important factor in their high in vivo analgesic potencies. Their enhanced resistance to peptidase degradation improves the distribution of the analogues within the blood and the CNS, so that the peptides are able to reach their target receptor on the membrane and produce their analgesic effect. It has been reported that the introduction of β-amino acids enhances

peptide stability;[34,56−58] therefore, we believed that the βPro[2] and Map substitutions are the main factors underlying the increased metabolic stability.

The potent antinociceptive effect of the investigated analogues following peripheral administration indicates the ability of the analogues to cross the highly selective BBB. To further evaluate the action site, a peripheral-restricted opioid receptor antagonist, naloxone methiodide, was injected intraperitoneally. The antagonist failed to produce any obvious inhibitory effect on the iv injected analogues. Collectively, these results confirm that the tested analogues were able to cross the BBB and that their antinociceptive effects were exerted primarily in the CNS. The incorporation of the unnatural amino acids Dmt[1] and βPro[2] resulted in an increase of bioactivity; however, such modifications only provided the peptide with limited access to the CNS.[10] We propose that introduction of the highly constrained residue, Map, was mainly responsible for the enhanced BBB penetration of the peptides. Limitation of the conformational flexibility was regarded as an efficient strategy for BBB permeability.[59]

The interaction characteristics between the analogues and MOR were further investigated by computational modeling methods. The two modeled analogues occupied the pocket formed by Asp147, Tyr148, Glu229, His223, and Trp318, which have been identified as key residues for ligand binding in site-directed mutagenesis studies.[60−66] This finding indicates that the established binding modes of the two analogues were in line with previous experimental data. Although analogues **10** and **12** showed similar overall orientation in the binding pocket, different binding modes were observed in the local area, particularly in position 4. The furan ring of (2-furyl)Map[4] is believed to be an important group that would form a hydrogen bond with the receptor and thus stabilizes the peptide conformation in the binding pocket.[41] This hydrogen bond was preserved in analogue **12** with His223. However, the introduction of (S)-βPro[2] into analogue **10** resulted a spatial shift of (2-furyl)Map[4], and the peptide lost its H-bond with His223. As a consequence, analogue **10** did not interact with the receptor as robustly as analogue **12**. These results explain the higher affinity of analogue **12** for the MOR and the similar affinity between analogues **9** and **10**. The molecular modeling data further confirm that the stereochemical feature of βPro is crucial in determining the binding conformation of the peptide.

CONCLUSION

In the current study, a new series of EM-1 analogues, carrying multiple structural modifications, were synthesized to enhance pharmacological activity and stability. The analogues exhibited high MOR activities at the MOR and significantly improved metabolic stability. The chirality and the aromatic properties of the incorporated β-amino acids play important roles in determining both the activity and selectivity of the peptides. The combined incorporation of Dmt[1], (*R*)-βPro[2], and (ph)-Map/(2-furyl)Map[4] into EM-1 resulted in the two most potent analogues with picomolar affinity and subpicomolar potency for MOR, which were far more potent than their parent peptide. In vivo assays also showed that these two analogues possessed enhanced antinociceptive activities and an improved ability to cross the BBB. Additionally, because both (*R*/*S*)-βPro and Map could be considered as β-amino acids, our work further emphasizes the application of β-amino acids in EM modification. These novel EM-1 analogues may serve as valuable compounds in pharmacological research for novel, clinically useful analgesic drugs.

EXPERIMENTAL SECTION

Materials and Methods. All standard amino acids and (*R*/*S*)-β-proline were commercially available, whereas the chiral 2-methylene-3-amino propanoic acids (Map) were prepared as in our previous reports.[41] Mass spectra were measured with a Maxis 4G ESI-TOF analyzer (Bruker, Fremont, CA). Melting points were determined on a micromelting point apparatus (AII-E, China). Purities were determined by ascending TLC performed on precoated plates and by analytical RP-HPLC. The purity of the analogues was confirmed by ascending TLC performed on precoated plates (silica gel 60 F254, Yinlong, China) in the following solvent systems (all v:v): (I) ethyl acetate−methanol−ammonia water (30:10:1), (II) acetone−glacial acetic acid−water (10:1:1). UV light and I_2 vapor were applied to visualize the TLC spots. Analytical RP-HPLC was carried out with a Waters Delta 600 instrument equipped with a Waters Deltapak C18 column (4.6 mm × 250 mm, 5 μm); absorbance was monitored at λ = 220 nm. The solvents for analytical RP-HPLC were as follows: A, 0.1% TFA in acetonitrile; B, 0.1% TFA in water. The column was eluted at a flow rate of 1 mL/min with a linear gradient of A:B = 10:90 to A:B = 90:10 for 30 min, and a gradient of A:B = 90:10 to A:B = 10:90 for 5 min. The retention time was reported as t_R (min). The final purity of the analogues was ≥95%. The detailed analytical properties of the synthetic analogues were provided in Table 1.

[^{3}H]DAMGO (50 Ci/mmol), [^{3}H]DPDPE (43 Ci/mmol), [^{3}H]-U69,593 (43.6 Ci/mmol), and [^{3}H] cAMP (50 Ci/mmol) were purchased from Perkin-Elmer (Boston, MA). Antiphospho-ERK1/2 (Thr202/Tyr204) antibodies, anti-ERK1/2 antibodies, and HRP-conjugated secondary antibody were purchased from Cell Signaling Technology Inc. Protein kinase A, forskolin, and IBMX were the products of Sigma-Aldrich (St. Louis, MO). The radioactivities were measured by a Perkin-Elmer Precisely 2460 Microplate Counter. The scintillation cocktail was obtained from Perkin-Elmer.

Animals. Guinea pigs (300−350 g, National Institute of the Biological Products, Gansu, People's Republic of China) were used for the guinea pig ileum (GPI) assay, male Kunming mice (30−35 g, Animal Center of Medical College of Lanzhou University, Gansu, People's Republic of China) were used for the mouse vas deferens (MVD) assay, and male Kunming mice (18−22 g, Animal Center of Medical College of Lanzhou University, Gansu, People's Republic of China) were employed for analgesia studies.

Animal were housed in a temperature-controlled environment (22 ± 2 °C) under standard 12 h light/dark conditions and received food and water ad libitum. All animals received care, and experiments were carried out in accordance with the principles and guidelines of the American Council on Animal Care. All protocols were approved by the Ethics Committee of Lanzhou Medical College, China.

Peptide Synthesis. Endomorphins and their analogues were obtained by solution-phase methods with segment-coupling peptide synthesis strategy as described previously.[41] Synthesis of all the peptides has been accomplished by performing an active ester reaction with the EDC/HOBt coupling method as described below.

The synthesis of the peptides begins with the coupling between Boc-Trp-OH and H-Map-NH_2 to obtain C-terminal dipeptides. The amide of Map was easily achieved by EDC/HOBt coupling with ammonia. The dipeptides were deprotected in HCl/EA (1:4). Using the same methods, Boc-Tyr/Dmt-OH and H-Pro/(R/S)βPro-ONa were coupled to obtain N-terminal dipeptides. After the synthesis of fragments, the active ester method using EDC/HOBt as the coupling agents resulted in the N- and C-terminal fragment coupling. The Boc group was removed by HCl in EA to give the final products. All the intermediates were characterized by TLC, ^{1}H NMR, and ESI-TOF MS. Final products were purified by semipreparative RP-HPLC and were 95−99% pure as determined by analytical RP-HPLC.

Cell Culture. HEK293 cells stably expressing either the FLAG-tagged-μ-opioid receptor or the Myc-tagged-δ-opioid receptor were grown in Dulbecco's modified Eagle's medium (DMEM) supple-

mented with 10% fetal calf serum, 100 units/mL penicillin, and 0.1 mg/mL streptomycin, at 37 °C in a humidified atmosphere containing 5% CO_2 as described.[67] Establishment of HEK293 cells stably expressing μ- or δ-opioid receptors is shown in Supporting Information (Figure S1).

Radioligand Binding Assay. The detailed description of competition binding experiments was described previously.[41] In the experiments designed to define peptide specificity for μ-, δ-, and κ-opioid receptors, whole cells expressing either MOR, DOR, or KOR ($2.5-3.5 \times 10^6$ cells/tube) were incubated with 1.7 nM [^{3}H]DAMGO, 1.0 nM [^{3}H]DPDPE, or 2.0 nM [^{3}H]U69,593 and 10^{-10} to 10^{-4} M unlabeled ligands for each experiment. Nonspecific binding was measured in the presence of 10 μM naloxone, 10 μM naltrexone, or 10 μM nor-BNI. The reaction was performed in 25 °C for 60 min in freshly prepared binding buffer (25 mM HEPES, 5 mM $MgCl_2$, 1 mM $CaCl_2$, 2.5 mM ethylenediaminetetraacetic acid [EDTA], and 0.4% bovine serum albumin [BSA], pH 7.4).[68,69] The reaction was stopped by rapid vacuum filtration through GF/C filters (Whatman, Maidstone, U.K.) using a cell harvester. The filters were washed twice with 6 mL of ice-cold buffer and then dried for 1 h at 80 °C. The radioactivity was measured by liquid scintillation counting (liquid scintillation counter, PerkinElmer). The affinity constants (K_i) were calculated according to Cheng and Prusoff with GraphPad Prism 5.0 software (GraphPad Software Inc., San Diego, CA). The dissociation constant (K_d^{μ} = 0.6 nM, K_d^{δ} = 2.8 nM, K_d^{κ} = 2.9 nM) and the number of binding sites (B_{max}) were calculated by Scatchard analysis using at least seven concentrations of [^{3}H]DAMGO, [^{3}H]DPDPE, or [^{3}H]U69,593 in a range of 0.085–8.5 nM, 0.10–5.05 nM, or 0.10–5.00 nM. Nonspecific binding was assessed in the presence of 10 μM naloxone, 10 μM naltrexone, and 10 μM nor-BNI.

Measurements of cAMP Accumulation. The assay was performed according to the procedure described elsewhere.[70−73] Briefly, the day before the assay, HEK293 cells stably expressing the μ-opioid receptor were seeded at 80% confluency in 24-well microtiter plates. Before beginning the assay, the culture medium was aspirated and each well was washed twice with serum-free medium warmed to 37 °C. Prewarmed serum-free medium (400 μL) containing 1 mM IBMX was added to each well and incubated 10 min at 37 °C. A 100 μL amount of serum-free medium containing various concentrations of the appropriate ligand (5×10^{-11} M to 5×10^{-5} M) using 50 μM forskolin was added to the cells and incubated at 37 °C for 30 min. The medium was removed, and then 0.2 N HCl was added to the cells at room temperature for 30 min. The clarified lysates were neutralized with 10 N NaOH. Lysates were transferred to microcentrifuge tubes and microcentrifuged 2 min at top speed at room temperature. Then 50 μL of neutralized lysates, 100 μL of PKA (60 μg/mL), and 50 μL of [^{3}H] cAMP were mixed briefly and incubated ≥2 h at 4 °C. The chilled charcoal suspension was added to adsorb free cAMP from solutions. A 200 μL amount of the supernatant was transferred to a scintillation vial. Scintillation fluid was added, and radioactivity was quantified in a scintillation counter (liquid scintillation counter, PerkinElmer). Analysis of the data was performed using the Graph-Pad Prism software (version 5.0, San Diego, CA).

Detection of MAPK Phosphorylation. The detailed description of detection of MAPK phosphorylation was described previously.[74−76] HEK293 cells stably expressing the FLAG-tagged-μ-opioid receptor were seeded in 12-well plates. Sixteen hours before the addition of the ligands, the culture medium was removed and replaced by fresh serum-free medium. For a rapid ERK1/2 phosphorylation assay, the cells were treated with analogues and incubated at 37 °C for 10 min. Cell monolayers were rinsed with ice-cold PBS, and whole lysates were prepared by the addition of RIPA lysis buffer containing 10 μM PMSF and phosphatase inhibitor cocktails (P5726, Sigma-Aldrich) for 5 min. Soluble proteins were separated by centrifugation at 15 000 rpm for 10 min. Protein concentration was determined by using a BCA protein assay kit (Pierce, Thermo Scientific, Rockford, IL). A 20 μg amount of protein from each sample was prepared for 10% SDS-polyacrylamide gel electrophoresis and electroblotted onto polyvinylidene difluoride membranes. Membranes were probed with primary antibody against phosphor-ERK1/2 or ERK1/2 (1:1000 dilution in blocking solution, Cell Signaling Technology Inc.). Immunoreactive proteins were visualized using a horseradish peroxidase-sensitive ECL chemiluminescent Western blotting kit (Pierce, Thermo Scientific).

In Vitro Assays on Isolated Tissue Preparation. In vitro opioid activities of peptides were tested in the guinea pig ileum (GPI) and mouse vas deferens (MVD) bioassays.[77] For the GPI assay, the myenteric plexus longitudinal muscle was obtained from guinea pig (300–350 g, National Institute of the Biological Products, Gansu, People's Republic of China) as reported elsewhere.[78] For the MVD assay, the vas deferens of male Kunming strain mice (30–35 g, Animal Center of Medical College of Lanzhou University, Gansu, People's Republic of China) was prepared as described previously.[79] The GPI tissue and MVD tissues were mounted in a 10 mL bath containing aerated (95% O_2, 5% CO_2) Krebs–Henseleit solution at 37 °C and 36 °C, respectively. Both tissues were used for field stimulation with bipolar rectangular pulses of supramaximal voltage. Dose–response curves were constructed, and IC_{50} values (concentration causing a 50% decrease in electrically induced twitches) were calculated graphically. Moreover, in both assays, three to four washings were performed with intervals of 15 min between each dose. The values were arithmetic means of 10–15 measurements. To measure whether δ-opioid receptor-mediated antagonism occurred in the MVD, naltrindole, a selective δ-receptor antagonist, was added to the tissue preparation, and after 5 min incubation, the test analogue was added at the IC_{50} dose value. The percentage recovery (reversal rate) of electrically evoked contraction was then calculated.

Metabolic Stability. The degradation studies of the endomorphin analogues were performed as described in detail previously.[80] The protein content of the suspension was confirmed with a BCA protein assay kit (Thermo, Rockford, IL). A final protein concentration of 2.1 mg/mL in 50 mM Tris buffer, pH 7.4, was used for all incubations. RP-HPLC analysis determined the stability of the peptides. Approximately 10 μL of peptide stock solution was digested with 190 μL of rat brain homogenate at 37 °C at a final volume of 200 μL for incubation. A 20 μL aliquot was withdrawn from the mixture at 0, 10, 30, 60, 120, 240, 480 min, and 90 μL of acetonitrile was added immediately to precipitate proteins.The tube was placed on ice for 5 min, and 90 μL of 0.5% acetic acid was added at the required time to prevent further enzymatic breakdown. The aliquots were centrifuged at 13 000g for 15 min at 4 °C. The obtained supernatants were filtered, and 50 μL of the filtrate was analyzed by RP-HPLC on a Waters Delta Pak C18 column (4.6 mm × 250 mm, Milford, MA). Using the solvent system of 0.1% TFA in acetonitrile (A) and 0.1% TFA in water (B) with a linear gradient of A:B = 10:90 to A:B = 90:10 for 30 min and A:B = 90:10 to A:B = 10:90 for 5 min, the column was eluted at a flow rate of 0.8 mL/min. The degradation rate constants (k) were determined by least-squares linear regression analysis of the logarithmic tetrapeptide peak area [$(\ln(A_t/A_0)$] vs time courses, with at least seven time points. The rate constants obtained were used to establish the degradation half-lives ($t_{1/2}$) as ln $2/k$.

Antinociception Test. The nociceptive response was assessed by the warm water tail-flick test as reported previously.[44] For the analgesia studies, male Kunming mice weighing 18–22 g were employed, and they were obtained from the Animal Center of Medical College of Lanzhou University. Various doses of drugs were injected icv according to the procedure adopted by Haley and McCormick, and the warm water tail-flick responses were measured at different times after the injection.[81] For iv injections, the analogues were injected at the same doses. For the study involving the opioid antagonist, animals were pretreated with naloxone both centrally and peripherally before iv challenge with peptides. We also evaluated the antagonist effect of naloxone methiodide, which does not readily cross the BBB.

Nociception was evoked by immersing the mouse tail in hot water (50 ± 0.2 °C) and measuring the latency to withdrawal. Before treatment, each mouse was tested, the latency to tail-flick [control latency (CL)] was recorded, and those with a latency of approximately 3–5 s were selected. The latency to tail-flick was defined as the test latency (TL), the corresponding cutoff time TL was set at 10 s, and 0.9% saline was used as control. The antinociceptive response was expressed as the percentage of maximal possible effect (%MPE),

calculated by the following equation: %MPE = 100 × (TL − CL)/(10 − CL). The data from each animal were converted to the area under the curve (AUC). We calculated the AUC data over a period of 0−60 min. The area under the curves depicting total %MPE versus time was computed by trapezoidal approximation over a period of 0−60 min.

Molecular Modeling. The MOR model built by Mosberg was used because this model represented the "active" state of the MOR and was proved to be suitable for peptide agonist binding.[64,82] The model was then refined using a 15-ns MD simulation in the phospholipid bilayer. MD simulations were performed with the GROMACS 3.3.3 package employing NPT and periodic boundary conditions.[83] A modification of GROMOS87 force field was applied for protein and the lipid.[84] The Particle Mesh Ewald algorithm was used for the calculation of electrostatic contributions to energies and forces.[85] Bond length was constrained using the LINCS algorithm.[86] The systems were coupled to a temperature bath at 300 K, with a coupling constant of 0.1 ps. Semiisotropic coupling with a time constant of 1 ps was applied to keep the pressure at 1.0 bar.[87] The system was first energy minimized using the steepest descent integrator for 5000 steps. Then a progression of position restraint was performed for 300 ps. Finally, a 15-ns simulation was performed with a time step of 2 fs. The average structure of the last 1 ns trajectory was considered as the typical structure of the MD simulations.

The molecular dockings were performed with the AUTODOCK4.[88] The initial conformations of the three analogues were built based on the NMR structure of endomorphins which we solved previously,[77] and the amide group of Tyr^1 was protonated. The docking process was performed in two steps.[89,90] First, a box of 42 × 42 × 42 Å, centered on one of the oxygen atoms of the Asp147, was used with a grid resolution of 5.5 Å. The population size was 100, the maximum number of generations was 27 000, and the maximum number of energy evaluations was 2 500 000. The lowest docking energy conformations or the lowest docking energy conformations included in the largest cluster were considered to be the most stable orientations. In the second step, a box of 40 × 30 × 50 Å, centered on the best conformations obtained in the first step, was used with a resolution of 0.3 Å. The number of energy evaluations was changed to 25 000 000, and the population size was raised to 500. The resulting orientations were scored based on the docking and binding energies and on the distance of Asp147 to the protonated nitrogen of the ligand. This residue was believed to be the primary binding site.[60] The docked energies were calculated using a modified scoring function.[91] In the next stage of the study, MD simulations of the all the docking models were performed using the GROMACS program to get more reasonable ligand−receptor binding modes. Each ligand−receptor complex was subjected to a 5 ns MD simulation in the previously described membrane bilayer. The RMSD value of each system is shown in Supporting Information (Figures S4 and S5). The topologies of the ligands were generated by PRODRG.[92] Figures were drawn by means of PyMOL.[93]

Data Analysis. The data are expressed as mean ± SEM. Responses were analyzed with a one-way ANOVA followed by Dunnett's test for comparison of multiple groups with one saline control group, and Student's t test for comparisons between two groups ($p < 0.05$ was used as the statistical significance level).

■ ASSOCIATED CONTENT

Supporting Information

Experimental details and characterization data for new analogues. This material is available free of charge via the Internet at http://pubs.acs.org.

■ AUTHOR INFORMATION

Corresponding Author

*Phone: +86-9318912567. E-mail: wangrui@lzu.edu.cn.

Author Contributions

‡These authors contributed equally.

Notes

The authors declare no competing financial interest.

■ ACKNOWLEDGMENTS

We are grateful for the grants from the National Natural Science Foundation of China (nos. 91213302, 20932003, and 21272102), the Key National S&T Program "Major New Drug Development" of the Ministry of Science and Technology of China (2012ZX09504001-003), and Fundamental Research Funds for the Central Universities (grant lzujbky-2011-86). We acknowledge computing resources and time in the Gansu Supercomputing Center, Cold and Arid Environment and Engineering Research Institute of Chinese Academy of Sciences, and Scholarship Award for Excellent Doctoral Student granted by the Ministry of Education.

■ ABBREVIATIONS USED

AUC, area under the curve; BBB, blood−brain barrier; Boc, *tert*-butyloxycarbonyl; cAMP, cyclic adenosine monophosphate; CNS, central nervous system; DAMGO, H-Tyr-D-Ala-Gly-*N*MePhe-Gly-ol; DCM, dichloromethane; DIEA, *N*,*N*′-diisopropylethylamine; DMF, dimethylformamide; Dmt, 2′,6′-dimethyltyrosine; DMSO, dimethyl sulfoxide; DOR, δ-opioid receptor; DPDPE, Tyr-c(D-Pen-Gly-Phe-D-Pen); ED_{50}, median effective dose; EDC, *N*-ethyl-*N*′-(3-(dimethylamino)propyl)-carbodiimide; EM-1, endomorphin-1; EM-2, endomorphin-2; ERK, extracellular regulated kinases; ESI-TOF MS, electrospray ionization time-of-flight mass spectrometry; GPI, guinea pig ileum; HEK293, human embryonic kidney; HOBt, 1-hydroxybenzotriazole; IC_{50}, 50% inhibitory concentration; icv, intracerebroventricular; ip, intraperitoneally; iv, intravenous; KOR, κ-opioid receptor; Map, α-methylene-β-aminopropanoic acids; MOR, μ-opioid receptor; MVD, mouse vas deferens; RP-HPLC, reversed-phase high performance liquid chromatography; SAR, structure−activity relationship; THF, tetrahydrofuran; TLC, thin-layer chromatography

■ REFERENCES

(1) Holden, J. E.; Jeong, Y.; Forrest, J. M. The endogenous opioid system and clinical pain management. *AACN Clin. Issues* **2005**, *16*, 291−301.

(2) Janecka, A.; Fichna, J.; Janecki, T. Opioid receptors and their ligands. *Curr. Top. Med. Chem.* **2004**, *4*, 1−17.

(3) Benyamin, R.; Trescot, A. M.; Datta, S.; Buenaventura, R.; Adlaka, R.; Sehgal, N.; Glaser, S. E.; Vallejo, R. Opioid complications and side effects. *Pain Physician* **2008**, *11*, S105−120.

(4) Davis, M. P. Opioid receptor targeting ligands for pain management: a review and update. *Expert Opin. Drug Dis.* **2010**, *5*, 1007−1022.

(5) Zadina, J. E.; Hackler, L.; Ge, L. J.; Kastin, A. J. A potent and selective endogenous agonist for the mu-opiate receptor. *Nature* **1997**, *386*, 499−502.

(6) Hackler, L.; Zadina, J. E.; Ge, L. J.; Kastin, A. J. Isolation of relatively large amounts of endomorphin-1 and endomorphin-2 from human brain cortex. *Peptides* **1997**, *18*, 1635−1639.

(7) Vaccarino, A. L.; Kastin, A. J. Endogenous opiates: 2000. *Peptides* **2001**, *22*, 2257−2328.

(8) Wilson, A. M.; Soignier, R. D.; Zadina, J. E.; Kastin, A. J.; Nores, W. L.; Olson, R. D.; Olson, G. A. Dissociation of analgesic and rewarding effects of endomorphin-1 in rats. *Peptides* **2000**, *21*, 1871−1874.

(9) Czapla, M. A.; Gozal, D.; Alea, O. A.; Beckerman, R. C.; Zadina, J. E. Differential cardiorespiratory effects of endomorphin 1, endomorphin 2, DAMGO, and morphine. *Am. J. Respir. Crit. Care Med.* **2000**, *162*, 994−999.

(10) Liu, W. X.; Wang, R. Endomorphins: potential roles and therapeutic indications in the development of opioid peptide analgesic drugs. *Med. Res. Rev.* **2012**, *32*, 536−580.
(11) Keresztes, A.; Borics, A.; Toth, G. Recent advances in endomorphin engineering. *ChemMedChem* **2010**, *5*, 1176−1196.
(12) Tomboly, C.; Peter, A.; Toth, G. In vitro quantitative study of the degradation of endomorphins. *Peptides* **2002**, *23*, 1573−1580.
(13) Mentlein, R. Dipeptidyl-peptidase IV (CD26)–role in the inactivation of regulatory peptides. *Regul. Pept.* **1999**, *85*, 9−24.
(14) Shane, R.; Wilk, S.; Bodnar, R. J. Modulation of endomorphin-2-induced analgesia by dipeptidyl peptidase IV. *Brain Res.* **1999**, *815*, 278−286.
(15) Janecka, A.; Staniszewska, R.; Gach, K.; Fichna, J. Enzymatic degradation of endomorphins. *Peptides* **2008**, *29*, 2066−2073.
(16) Cardillo, G.; Gentilucci, L.; Tolomelli, A. Unusual amino acids: synthesis and introduction into naturally occurring peptides and biologically active analogues. *Mini-Rev. Med. Chem.* **2006**, *6*, 293−304.
(17) Schwyzer, R. ACTH: a short introductory review. *Ann. N.Y. Acad. Sci.* **1977**, *297*, 3−26.
(18) In, Y.; Minoura, K.; Ohishi, H.; Minakata, H.; Kamigauchi, M.; Sugiura, M.; Ishida, T. Conformational comparison of mu-selective endomorphin-2 with its C-terminal free acid in DMSO solution, by ^{1}H NMR spectroscopy and molecular modeling calculation. *J. Pept. Res.* **2001**, *58*, 399−412.
(19) Berezowska, I.; Chung, N. N.; Lemieux, C.; Wilkes, B. C.; Schiller, P. W. Agonist vs antagonist behavior of δ opioid peptides containing novel phenylalanine analogues in place of Tyr(1). *J. Med. Chem.* **2009**, *52*, 6941−6945.
(20) Tomboly, C.; Ballet, S.; Feytens, D.; Kover, K. E.; Borics, A.; Lovas, S.; Al-Khrasani, M.; Furst, Z.; Toth, G.; Benyhe, S.; Tourwe, D. Endomorphin-2 with a β-turn backbone constraint retains the potent μ-opioid receptor agonist properties. *J. Med. Chem.* **2008**, *51*, 173−177.
(21) Janecka, A.; Kruszynski, R. Conformationally restricted peptides as tools in opioid receptor studies. *Curr. Med. Chem.* **2005**, *12*, 471−481.
(22) Janecka, A.; Staniszewska, R.; Fichna, J. Endomorphin analogs. *Curr. Med. Chem.* **2007**, *14*, 3201−3208.
(23) Schiller, P. W. Bi- or multifunctional opioid peptide drugs. *Life Sci.* **2010**, *86*, 598−603.
(24) Gentilucci, L.; Tolomelli, A. Recent advances in the investigation of the bioactive conformation of peptides active at the mu-opioid receptor. conformational analysis of endomorphins. *Curr. Top. Med. Chem.* **2004**, *4*, 105−121.
(25) Hruby, V. J.; Balse, P. M. Conformational and topographical considerations in designing agonist peptidomimetics from peptide leads. *Curr. Med. Chem.* **2000**, *7*, 945−970.
(26) Hruby, V. J.; Porreca, F.; Yamamura, H. I.; Tollin, G.; Agnes, R. S.; Lee, Y. S.; Cai, M.; Alves, I.; Cowell, S.; Varga, E.; Davis, P.; Salamon, Z.; Roeske, W.; Vanderah, T.; Lai, J. New paradigms and tools in drug design for pain and addiction. *AAPS J.* **2006**, *8*, E450−460.
(27) Torino, D.; Mollica, A.; Pinnen, F.; Feliciani, F.; Lucente, G.; Fabrizi, G.; Portalone, G.; Davis, P.; Lai, J.; Ma, S. W.; Porreca, F.; Hruby, V. J. Synthesis and evaluation of new endomorphin-2 analogues containing (Z)-α,β-didehydrophenylalanine (δ(Z)Phe) residues. *J. Med. Chem.* **2010**, *53*, 4550−4554.
(28) Giordano, C.; Sansone, A.; Masi, A.; Lucente, G.; Punzi, P.; Mollica, A.; Pinnen, F.; Feliciani, F.; Cacciatore, I.; Davis, P.; Lai, J.; Ma, S. W.; Porreca, F.; Hruby, V. Synthesis and activity of endomorphin-2 and morphiceptin analogues with proline surrogates in position 2. *Eur. J. Med. Chem.* **2010**, *45*, 4594−4600.
(29) Bryant, S. D.; Jinsmaa, Y.; Salvadori, S.; Okada, Y.; Lazarus, L. H. Dmt and opioid peptides: a potent alliance. *Biopolymers* **2003**, *71*, 86−102.
(30) Schiller, P. W. Opioid peptide-derived analgesics. *AAPS J.* **2005**, *7*, E560−565.
(31) Seebach, D.; Overhand, M.; Kühnle, F.; Martinoni, B.; Oberer, L.; Hommel, U.; Widmer, H. β-Peptides: Synthesis by *Arndt-Eistert* homologation with concomitant peptide coupling. Structure determination by NMR and CD spectroscopy and by X-ray crystallography. Helical secondary structure of a β-hexapeptide in solution and its stability towards pepsin. *Helv. Chim. Acta* **1996**, *79*, 913−941.
(32) Appella, D. H.; Christianson, L. A.; Karle, I. L.; Powell, D. R.; Gellman, S. H. β-Peptide foldamers: Robust helix formation in a new family of β-amino acid oligomers. *J. Am. Chem. Soc.* **1996**, *118*, 13071−13072.
(33) Steer, D. L.; Lew, R. A.; Perlmutter, P.; Smith, A. I.; Aguilar, M. I. Beta-amino acids: versatile peptidomimetics. *Curr. Med. Chem.* **2002**, *9*, 811−822.
(34) Keresztes, A.; Szucs, M.; Borics, A.; Kover, K. E.; Forro, E.; Fulop, F.; Tomboly, C.; Peter, A.; Pahi, A.; Fabian, G.; Muranyi, M.; Toth, G. New endomorphin analogues containing alicyclic β-amino acids: influence on bioactive conformation and pharmacological profile. *J. Med. Chem.* **2008**, *51*, 4270−4279.
(35) Perlikowska, R.; Gach, K.; Fichna, J.; Toth, G.; Walkowiak, B.; do-Rego, J. C.; Janecka, A. Biological activity of endomorphin and [Dmt1]endomorphin analogs with six-membered proline surrogates in position 2. *Bioorg. Med. Chem.* **2009**, *17*, 3789−3794.
(36) Staniszewska, R.; Fichna, J.; Gach, K.; Toth, G.; Poels, J.; Vanden Broeck, J.; Janecka, A. Synthesis and biological activity of endomorphin-2 analogs incorporating piperidine-2-, 3- or 4-carboxylic acids instead of proline in position 2. *Chem. Biol. Drug. Des.* **2008**, *72*, 91−94.
(37) Torino, D.; Mollica, A.; Pinnen, F.; Lucente, G.; Feliciani, F.; Davis, P.; Lai, J.; Ma, S. W.; Porreca, F.; Hruby, V. J. Synthesis and evaluation of new endomorphin analogues modified at the Pro(2) residue. *Bioorg. Med. Chem. Lett.* **2009**, *19*, 4115−4118.
(38) Frackenpohl, J.; Arvidsson, P. I.; Schreiber, J. V.; Seebach, D. The outstanding biological stability of beta- and gamma-peptides toward proteolytic enzymes: an in vitro investigation with fifteen peptidases. *ChemBioChem* **2001**, *2*, 445−455.
(39) Cheng, R. P.; Gellman, S. H.; DeGrado, W. F. β-Peptides: From structure to function. *Chem. Rev.* **2001**, *101*, 3219−3232.
(40) Spampinato, S.; Qasem, A. R.; Calienni, M.; Murari, G.; Gentilucci, L.; Tolomelli, A.; Cardillo, G. Antinociception by a peripherally administered novel endomorphin-1 analogue containing beta-proline. *Eur. J. Pharmacol.* **2003**, *469*, 89−95.
(41) Wang, Y.; Xing, Y.; Liu, X.; Ji, H.; Kai, M.; Chen, Z.; Yu, J.; Zhao, D.; Ren, H.; Wang, R. A new class of highly potent and selective endomorphin-1 analogues containing α-methylene-β-aminopropanoic acids (map). *J. Med. Chem.* **2012**, *55*, 6224−6236.
(42) Zhao, D. P.; Yang, D. X.; Wang, Y. J.; Wang, Y.; Mao, L. J.; Wang, R. Enantioselective Mannich reaction of a highly reactive Horner-Wadsworth-Emmons reagent with imines catalyzed by a bifunctional thiourea. *Chem. Sci.* **2011**, *2*, 1918−1921.
(43) Li, T.; Fujita, Y.; Tsuda, Y.; Miyazaki, A.; Ambo, A.; Sasaki, Y.; Jinsmaa, Y.; Bryant, S. D.; Lazarus, L. H.; Okada, Y. Development of potent μ-opioid receptor ligands using unique tyrosine analogues of endomorphin-2. *J. Med. Chem.* **2005**, *48*, 586−592.
(44) Liu, H. M.; Liu, X. F.; Yao, J. L.; Wang, C. L.; Yu, Y.; Wang, R. Utilization of combined chemical modifications to enhance the blood-brain barrier permeability and pharmacological activity of endomorphin-1. *J. Pharmacol. Exp. Ther.* **2006**, *319*, 308−316.
(45) Sasaki, Y.; Sasaki, A.; Niizuma, H.; Goto, H.; Ambo, A. Endomorphin 2 analogues containing Dmp residue as an aromatic amino acid surrogate with high mu-opioid receptor affinity and selectivity. *Bioorg. Med. Chem.* **2003**, *11*, 675−678.
(46) Koda, Y.; Del Borgo, M.; Wessling, S. T.; Lazarus, L. H.; Okada, Y.; Toth, I.; Blanchfield, J. T. Synthesis and in vitro evaluation of a library of modified endomorphin 1 peptides. *Bioorg. Med. Chem.* **2008**, *16*, 6286−6296.
(47) Yabaluri, N.; Medzihradsky, F. Down-regulation of mu-opioid receptor by full but not partial agonists is independent of G protein coupling. *Mol. Pharmacol.* **1997**, *52*, 896−902.
(48) Liu, J. G.; Prather, P. L. Chronic agonist treatment converts antagonists into inverse agonists at delta-opioid receptors. *J. Pharmacol. Exp. Ther.* **2002**, *302*, 1070−1079.

(49) Hosohata, K.; Burkey, T. H.; Alfaro-Lopez, J.; Varga, E.; Hruby, V. J.; Roeske, W. R.; Yamamura, H. I. Endomorphin-1 and endomorphin-2 are partial agonists at the human mu-opioid receptor. *Eur. J. Pharmacol.* **1998**, *346*, 111−114.
(50) Sim, L. J.; Liu, Q.; Childers, S. R.; Selley, D. E. Endomorphin-stimulated [^{35}S]GTPγS binding in rat brain: evidence for partial agonist activity at μ-opioid receptors. *J. Neurochem.* **1998**, *70*, 1567−1576.
(51) Morou, E.; Georgoussi, Z. Expression of the third intracellular loop of the delta-opioid receptor inhibits signaling by opioid receptors and other G protein-coupled receptors. *J. Pharmacol. Exp. Ther.* **2005**, *315*, 1368−1379.
(52) Belcheva, M. M.; Szucs, M.; Wang, D.; Sadee, W.; Coscia, C. J. μ-Opioid receptor-mediated ERK activation involves calmodulin-dependent epidermal growth factor receptor transactivation. *J. Biol. Chem.* **2001**, *276*, 33847−33853.
(53) Fichna, J.; Perlikowska, R.; Wyrebska, A.; Gach, K.; Piekielna, J.; do-Rego, J. C.; Toth, G.; Kluczyk, A.; Janecki, T.; Janecka, A. Effect of 2′,6′-dimethyl-L-tyrosine (Dmt) on pharmacological activity of cyclic endomorphin-2 and morphiceptin analogs. *Bioorg. Med. Chem.* **2011**, *19*, 6977−6981.
(54) Asensio, V. J.; Miralles, A.; Garcia-Sevilla, J. A. Stimulation of mitogen-activated protein kinase kinases (MEK1/2) by mu-, delta- and kappa-opioid receptor agonists in the rat brain: regulation by chronic morphine and opioid withdrawal. *Eur. J. Pharmacol.* **2006**, *539*, 49−56.
(55) Ferrer-Alcon, M.; Garcia-Fuster, M. J.; La Harpe, R.; Garcia-Sevilla, J. A. Long-term regulation of signalling components of adenylyl cyclase and mitogen-activated protein kinase in the pre-frontal cortex of human opiate addicts. *J. Neurochem.* **2004**, *90*, 220−230.
(56) Cardillo, G.; Gentilucci, L.; Melchiorre, P.; Spampinato, S. Synthesis and binding activity of endomorphin-1 analogues containing beta-amino acids. *Bioorg. Med. Chem. Lett.* **2000**, *10*, 2755−2758.
(57) Cardillo, G.; Gentilucci, L.; Qasem, A. R.; Sgarzi, F.; Spampinato, S. Endomorphin-1 analogues containing β-proline are μ-opioid receptor agonists and display enhanced enzymatic hydrolysis resistance. *J. Med. Chem.* **2002**, *45*, 2571−2578.
(58) Mallareddy, J. R.; Borics, A.; Keresztes, A.; Kover, K. E.; Tourwe, D.; Toth, G. Design, synthesis, pharmacological evaluation, and structure−activity study of novel endomorphin analogues with multiple structural modifications. *J. Med. Chem.* **2011**, *54*, 1462−1472.
(59) Guillemyn, K.; Kleczkowska, P.; Novoa, A.; Vandormael, B.; Van den Eynde, I.; Kosson, P.; Asim, M. F.; Schiller, P. W.; Spetea, M.; Lipkowski, A. W.; Tourwe, D.; Ballet, S. In vivo antinociception of potent mu opioid agonist tetrapeptide analogues and comparison with a compact opioid agonist-neurokinin 1 receptor antagonist chimera. *Mol. Brain* **2012**, *5*, 4.
(60) Befort, K.; Tabbara, L.; Bausch, S.; Chavkin, C.; Evans, C.; Kieffer, B. The conserved aspartate residue in the third putative transmembrane domain of the delta-opioid receptor is not the anionic counterpart for cationic opiate binding but is a constituent of the receptor binding site. *Mol. Pharmacol.* **1996**, *49*, 216−223.
(61) Chen, C.; Yin, J.; Riel, J. K.; DesJarlais, R. L.; Raveglia, L. F.; Zhu, J.; Liu-Chen, L. Y. Determination of the amino acid residue involved in [^{3}H]beta-funaltrexamine covalent binding in the cloned rat mu-opioid receptor. *J. Biol. Chem.* **1996**, *271*, 21422−21429.
(62) Li, J. G.; Chen, C.; Yin, J.; Rice, K.; Zhang, Y.; Matecka, D.; de Riel, J. K.; DesJarlais, R. L.; Liu-Chen, L. Y. ASP147 in the third transmembrane helix of the rat mu opioid receptor forms ion-pairing with morphine and naltrexone. *Life Sci.* **1999**, *65*, 175−185.
(63) Mansour, A.; Taylor, L. P.; Fine, J. L.; Thompson, R. C.; Hoversten, M. T.; Mosberg, H. I.; Watson, S. J.; Akil, H. Key residues defining the mu-opioid receptor binding pocket: a site-directed mutagenesis study. *J. Neurochem.* **1997**, *68*, 344−353.
(64) Mosberg, H. I.; Fowler, C. B. Development and validation of opioid ligand-receptor interaction models: the structural basis of mu vs delta selectivity. *J. Pept. Res.* **2002**, *60*, 329−335.
(65) Surratt, C. K.; Johnson, P. S.; Moriwaki, A.; Seidleck, B. K.; Blaschak, C. J.; Wang, J. B.; Uhl, G. R. μ opiate receptor. Charged transmembrane domain amino acids are critical for agonist recognition and intrinsic activity. *J. Biol. Chem.* **1994**, *269*, 20548−20553.
(66) Shahrestanifar, M.; Wang, W. W.; Howells, R. D. Studies on inhibition of mu and delta opioid receptor binding by dithiothreitol and N-ethylmaleimide. His223 is critical for mu opioid receptor binding and inactivation by N-ethylmaleimide. *J. Biol. Chem.* **1996**, *271*, 5505−5512.
(67) Megaritis, G.; Merkouris, M.; Georgoussi, Z. Functional domains of delta- and mu-opioid receptors responsible for adenylyl cyclase inhibition. *Recept. Channels* **2000**, *7*, 199−212.
(68) Mitch, C. H.; Quimby, S. J.; Diaz, N.; Pedregal, C.; de la Torre, M. G.; Jimenez, A.; Shi, Q.; Canada, E. J.; Kahl, S. D.; Statnick, M. A.; McKinzie, D. L.; Benesh, D. R.; Rash, K. S.; Barth, V. N. Discovery of aminobenzyloxyarylamides as κ opioid receptor selective antagonists: Application to preclinical development of a κ opioid receptor antagonist receptor occupancy tracer. *J. Med. Chem.* **2011**, *54*, 8000−8012.
(69) Pinyot, A.; Nikolovski, Z.; Bosch, J.; Segura, J.; Gutierrez-Gallego, R. On the use of cells or membranes for receptor binding: growth hormone secretagogues. *Anal. Biochem.* **2010**, *399*, 174−181.
(70) Frandsen, E. K.; Krishna, G. A simple ultrasensitive method for the assay of cyclic AMP and cyclic GMP in tissues. *Life Sci.* **1976**, *18*, 529−541.
(71) Obermeier, H.; Wehmeyer, A.; Schulz, R. Expression of mu-, delta- and kappa-opioid receptors in baculovirus-infected insect cells. *Eur. J. Pharmacol.* **1996**, *318*, 161−166.
(72) Wei, Q.; Zhou, D. H.; Shen, Q. X.; Chen, J.; Chen, L. W.; Wang, T. L.; Pei, G.; Chi, Z. Q. Human mu-opioid receptor overexpressed in Sf9 insect cells functionally coupled to endogenous Gi/o proteins. *Cell Res.* **2000**, *10*, 93−102.
(73) Gusovsky, F. Measurement of second messengers in signal transduction: cAMP and inositol phosphates. *Current Protocols in Neuroscience*; Wiley: New York, 2001, Chapter 7, Unit 7.12.
(74) Korzh, A.; Keren, O.; Gafni, M.; Bar-Josef, H.; Sarne, Y. Modulation of extracellular signal-regulated kinase (ERK) by opioid and cannabinoid receptors that are expressed in the same cell. *Brain Res.* **2008**, *1189*, 23−32.
(75) Belcheva, M. M.; Clark, A. L.; Haas, P. D.; Serna, J. S.; Hahn, J. W.; Kiss, A.; Coscia, C. J. Mu and kappa opioid receptors activate ERK/MAPK via different protein kinase C isoforms and secondary messengers in astrocytes. *J. Biol. Chem.* **2005**, *280*, 27662−27669.
(76) Schmidt, H.; Schulz, S.; Klutzny, M.; Koch, T.; Handel, M.; Hollt, V. Involvement of mitogen-activated protein kinase in agonist-induced phosphorylation of the mu-opioid receptor in HEK 293 cells. *J. Neurochem.* **2000**, *74*, 414−422.
(77) Yu, Y.; Shao, X.; Cui, Y.; Liu, H. M.; Wang, C. L.; Fan, Y. Z.; Liu, J.; Dong, S. L.; Cui, Y. X.; Wang, R. Structure-activity study on the spatial arrangement of the third aromatic ring of endomorphins 1 and 2 using an atypical constrained C terminus. *ChemMedChem* **2007**, *2*, 309−317.
(78) Rang, H. P. Stimulant actions of volatile anaesthetics on smooth muscle. *Br. J. Pharmacol. Chemother.* **1964**, *22*, 356−365.
(79) Hughes, J.; Kosterlitz, H. W.; Leslie, F. M. Effect of morphine on adrenergic transmission in the mouse vas deferens. Assessment of agonist and antogonist potencies of narcotic analgesics. *Br. J. Pharmacol.* **1975**, *53*, 371−381.
(80) Gillespie, T. J.; Konings, P. N.; Merrill, B. J.; Davis, T. P. A specific enzyme assay for aminopeptidase M in rat brain. *Life Sci.* **1992**, *51*, 2097−2106.
(81) Wang, C. L.; Yao, J. L.; Yu, Y.; Shao, X.; Cui, Y.; Liu, H. M.; Lai, L. H.; Wang, R. Structure-activity study of endomorphin-2 analogs with C-terminal modifications by NMR spectroscopy and molecular modeling. *Bioorg. Med. Chem.* **2008**, *16*, 6415−6422.
(82) Liu, X.; Kai, M.; Jin, L.; Wang, R. Computational study of the heterodimerization between mu and delta receptors. *J. Comput.-Aided Mol. Des.* **2009**, *23*, 321−332.
(83) Berendsen, H. J.; Vanderspoel, D.; Vandrunen, R. GROMACS: A message-passing parallel molecular dynamics implementation. *Comput. Phys. Commun.* **1995**, *91*, 43−56.

(84) Vanbuuren, A. R.; Marrink, S. J.; Berendsen, H. J. C. A molecular dynamics study of the decane/water interface. *J. Phys. Chem.* **1993**, *97*, 9206−9212.
(85) Darden, T.; York, D.; Pedersen, L. Particle mesh Ewald: An *N*-log(*N*) method for Ewald sums in large system. *J. Chem. Phys.* **1993**, *98*, 10089−10092.
(86) Hess, B.; Bekker, H.; Berendsen, H. J. C.; Fraaije, J. LINCS: A linear constraint solver for molecular simulations. *J. Comput. Chem.* **1997**, *18*, 1463−1472.
(87) Berendsen, H. J. C.; Postma, J. P. M.; Vangunsteren, W. F.; Dinola, A.; Haak, J. R. Molecular dynamics with coupling to an external bath. *J. Chem. Phys.* **1984**, *81*, 3684−3690.
(88) Morris, G. M.; Goodsell, D. S.; Halliday, R. S.; Huey, R.; Hart, W. E.; Belew, R. K.; Olson, A. J. Automated docking using a Lamarckian genetic algorithm and an empirical binding free energy function. *J. Comput. Chem.* **1998**, *19*, 1639−1662.
(89) Hetenyi, C.; van der Spoel, D. Efficient docking of peptides to proteins without prior knowledge of the binding site. *Protein Sci.* **2002**, *11*, 1729−1737.
(90) Hetenyi, C.; van der Spoel, D. Blind docking of drug-sized compounds to proteins with up to a thousand residues. *FEBS Lett.* **2006**, *580*, 1447−1450.
(91) Hetenyi, C.; Paragi, G.; Maran, U.; Timar, Z.; Karelson, M.; Penke, B. Combination of a modified scoring function with two-dimensional descriptors for calculation of binding affinities of bulky, flexible ligands to proteins. *J. Am. Chem. Soc.* **2006**, *128*, 1233−1239.
(92) Schuttelkopf, A. W.; van Aalten, D. M. PRODRG: a tool for high-throughput crystallography of protein-ligand complexes. *Acta Crystallogr., Sect. D: Biol. Crystallogr.* **2004**, *60*, 1355−1363.
(93) DeLano, W. L. *The PyMOL Molecular Graphics System*, DeLano Scientific, Palo Alto, CA, 2002.